

Hazard analysis of tsunami disaster on the Maritime Silk Road

Jingming Hou^{1, 2, 3*}, Xiaojuan Li², Peitao Wang^{1, 3}, Juncheng Wang¹, Zhiyuan Ren¹

¹National Marine Environmental Forecasting Center, Beijing 100081, China

²College of Resource Environment and Tourism, Capital Normal University, Beijing 100048, China

³Key Laboratory of Research on Marine Hazards Forecasting, State Oceanic Administration, Beijing 100081, China

Received 21 December 2018; accepted 22 February 2019

© Chinese Society for Oceanography and Springer-Verlag GmbH Germany, part of Springer Nature 2020

Abstract

The Maritime Silk Road is not only a passageway for business and trade, but also the road of friendship between eastern and western civilizations. The Indian Ocean tsunami in 2004 caused major damage to several coastal countries. Tsunami occurrence regularity and hazard analysis are needed to ensure economic and cultural exchange on the Maritime Silk Road. To explore and identify tsunami hazard on the Maritime Silk Road, the spatial and temporal characteristics of historical tsunami events were given out. Some useful information hidden in historical tsunamis was searched from source parameters, such as seismic magnitude, focal depth and water depth. The tsunami possibility in the case of earthquake occurrence was also studied, exploring the probability of tsunami caused by different magnitudes. The analysis result shows that tsunamis on the Maritime Silk Road mainly occurred in 8 major tectonic faults, each of which has different tsunami occurrence regularity. On the basis of statistical analysis, a numerical model was used to simulate the potential tsunamis and show the tsunami hazard levels along the coast of Maritime Silk Road. The research results of this paper can help the tsunami early warning and ensure the safety of economic and cultural exchanges on the Maritime Silk Road.

Key words: tsunami, occurrence regularity, hazard, Maritime Silk Road

Citation: Hou Jingming, Li Xiaojuan, Wang Peitao, Wang Juncheng, Ren Zhiyuan. 2020. Hazard analysis of tsunami disaster on the Maritime Silk Road. *Acta Oceanologica Sinica*, 39(1): 74–82, doi: 10.1007/s13131-019-1526-z

1 Introduction

China proposed the 21st century Maritime Silk Road initiative in 2013 (Guan, 2016), which was welcomed and supported by many countries. This initiative aims to achieve harmonious coexistence and common development with relevant countries by revitalizing the ancient Maritime Silk Road. The Maritime Silk Road extends from China and Japan, through the South China Sea and the northern Indian Ocean, to East Africa and Europe, passing through more than 50 countries and regions. However, countries along the Maritime Silk Road often suffer from marine disasters. Tsunami is one of the most serious marine disasters in the world. In recent years, destructive tsunami has occurred every year (IOC, 2013). Since the beginning of the 21st century, there have been two major tsunamis on the Maritime Silk Road, the Indian Ocean tsunami (Grilli et al., 2007) in 2004 and the Japan tsunami (Wei et al., 2013) in 2011. Although tsunami is a low-probability event, its occurrence is often accompanied by huge economic loss and casualties (Wang et al., 2018). Moreover, tsunami can spread across the ocean and affect areas far from the source, causing widespread disasters (Hébert et al., 2001). Nowadays, scientists are still unable to predict when and where the next tsunami will occur. Therefore, it is necessary to study and analyze the tsunami events in advance to mitigate the disastrous effect of tsunami.

Tsunami could have disastrous effects on trade, shipping and other activities on the Maritime Silk Road. A number of organizations need to understand the tsunami hazard on the Maritime Silk Road to assess the safety of economic and cultural exchanges. Several published studies had analyzed the tsunami

hazard in China's surrounding waters (Liu et al., 2007; Wen et al., 2008; Dao et al., 2009). Regional tsunami assessments show the tsunami hazard of China's coastal provinces (Mao et al., 2015; Hou et al., 2016). The effect of China coastal topography on tsunamis has also been studied (Zhao et al., 2013). However, the tsunami hazard on the Maritime Silk Road has not been studied comprehensively. Although researchers have analyzed the historical tsunamis (Zhou and Adams, 1988), the occurrence regularity of tsunami disasters has not been clearly stated. In addition, the question of what kind of earthquake can trigger a tsunami has not been clarified.

This paper studied the temporal and spatial distribution and occurrence regularity of tsunamis on the Maritime Silk Road. The numerical model was used to simulate the potential tsunamis and identify the coastline with high tsunami risk. The analysis results are of great significance for ensuring the safety of economic and cultural exchanges on the Maritime Silk Road.

2 Spatiotemporal distribution of earthquakes and tsunamis

Most tsunamis are caused by earthquakes. Tsunami warning is initiated based on earthquake information. Once an earthquake occurs, the seismic wave data can be obtained first. According to the location and magnitude of the earthquake, the numerical model can be used to predict the tsunami travel time and wave amplitude. However, if the tsunami source is very close to the land, there may not be enough time to respond. So, it is necessary to have a comprehensive understanding of the occurrence of the submarine earthquakes and tsunamis on the Maritime Silk Road. In this study, the temporal and spatial distribu-

tions of earthquakes and tsunamis were analyzed using historical earthquake and tsunami data.

2.1 Analysis of historical earthquakes

The earthquake data (1917–2017) is from the global seismic database of the United States Geological Survey (USGS, 2018). Figure 1 shows the distribution of historical earthquakes on the Maritime Silk Road. From this figure we can see that earthquakes

are mostly distributed on plate boundaries. The northwestern Pacific Ocean and the northeastern Indian Ocean are the most seismically active areas, while there are fewer earthquakes in the mid-west Indian Ocean. The northwestern Pacific Ocean lies on the Circum-Pacific seismic belt, which is one of the world's major seismic zones. In addition, there are also large earthquakes occurring in the Mediterranean region, which belongs to another large seismic belt, the Eurasia seismic belt.

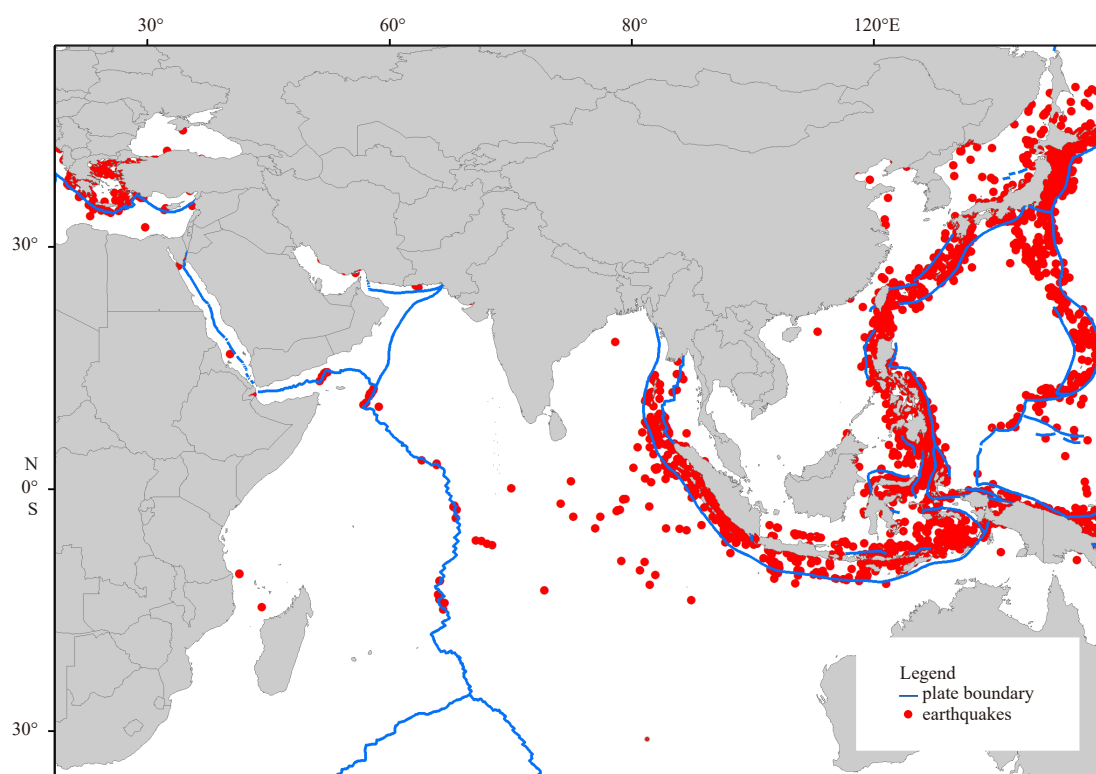


Fig. 1. Spatial distribution of earthquakes.

There are several large tectonic faults on the Maritime Silk Road, which are the sources of major earthquakes and tsunamis. Figure 2 shows 8 main faults on the Maritime Silk Road, including Japan Trench, Nankai Trough, Ryukyu Trench, Mariana Trench, Manila Trench, Philippine Trench, Java Trench and Hellenic Trench.

Figure 3 shows the annual earthquakes on the Maritime Silk Road between 1917 and 2017. As can be seen from this figure, the number of earthquakes fluctuated with time, with an peak every three years on average. In the 1950s, the number of earthquakes increased significantly. This is due to the invention and application of modern seismic monitoring equipment, which had improved the ability to monitor earthquakes. In the past 100 years, an average of 46 earthquakes with magnitude above 6 occurred annually along the Maritime Silk Road. The year of 2011 was the most frequent year with 121 earthquakes.

2.2 Analysis of historical tsunamis

To analyze the spatial and temporal variation of tsunami disasters on the Maritime Silk Road, this study selected tsunami data of past 100 years (1917–2017) from the Global Tsunami Database of National Geophysical Data Center (NGDC, 2018). Figure 4 reveals the spatial pattern of the tsunamis on the Maritime Silk Road. As can be seen from this figure, the tsunami

events also generally occurred on plate boundaries. The dense areas of the tsunami event are roughly the same as the intensive earthquake areas in Fig. 1. There are also some differences, such as the relatively smaller number of tsunami events in the Indian Ocean Ridge region. The areas with the most tsunami events include the Northwestern Pacific Ocean, the western waters of Sumatra, and the Mediterranean Sea.

The annual tsunami events (1917–2017) on the Maritime Silk Road is shown in Fig. 5. The annual number of tsunami events also fluctuated over time. In the past 100 a, an average of 4.8 tsunamis have been recorded annually on the Maritime Silk Road. The year of 1938 had the most tsunamis, 17 tsunamis.

2.3 Analysis of kernel density

Density analysis can help to understand the aggregation of earthquake and tsunami on the Maritime Silk Road. In this paper, the historical earthquake and tsunami events are analyzed by the method of kernel density. The kernel density analysis is the process of interpolation using discrete point (Cai et al., 2013). Each discrete point has different weights, and the points near the center have a larger weight. The algorithm used to determine the default search radius is as follows:

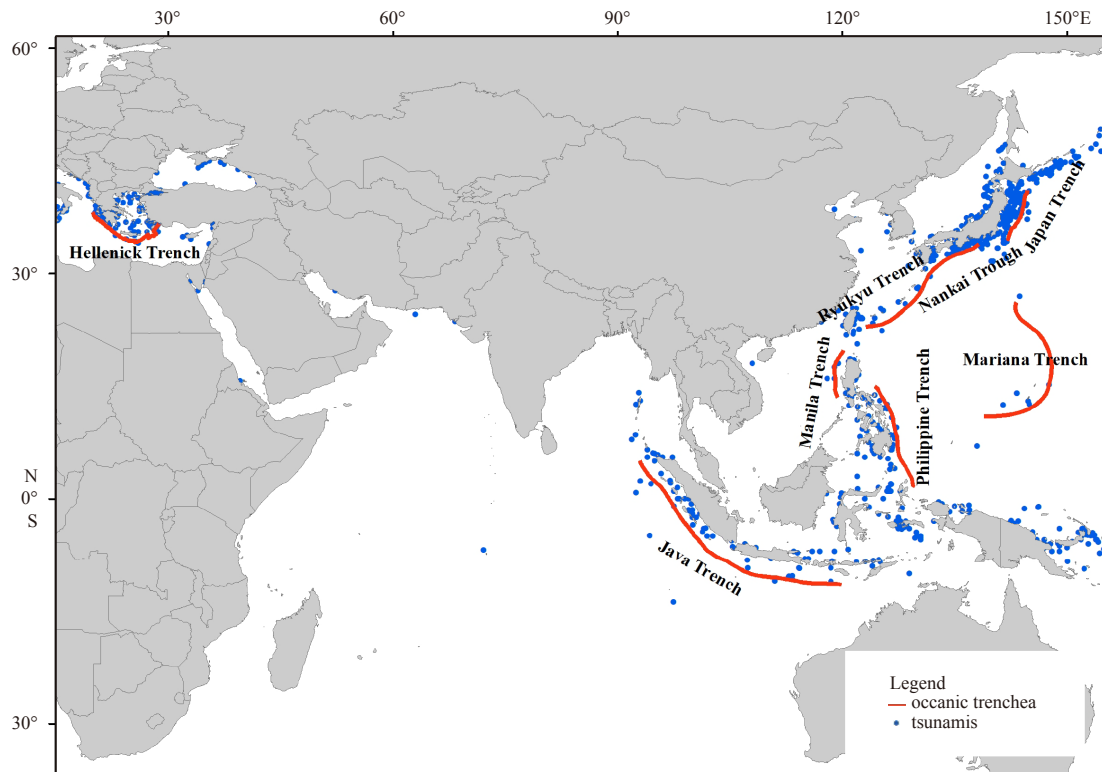


Fig. 2. Oceanic trenches along the Maritime Silk Road.

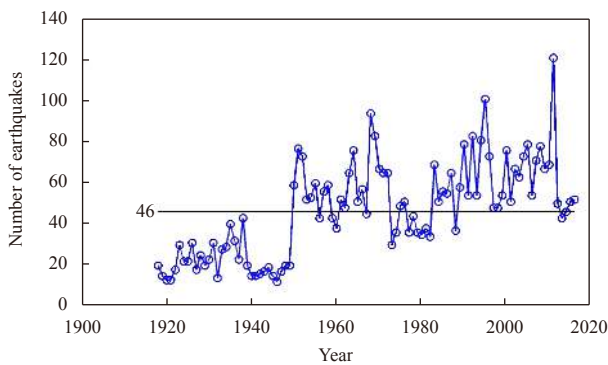


Fig. 3. Annual earthquakes on the Maritime Silk Road.

$$\text{search radius} = 0.9 \times \min \left(SD, \sqrt{\frac{1}{\ln(2)} \times D_m} \right) \times n^{-0.2}, \quad (1)$$

where SD is the standard distance, while n is the number of points. D_m represents the median distance. The search radius in this article is 126 km and the output resolution is 30 km. Density analysis was performed in ArcGIS software.

Figure 6 shows the kernel density analysis result of the historical earthquakes with magnitude above 6.0. From the results it can be seen that the most earthquake-intensive areas include the Japan-Taiwan-Philippines area and northwestern water of Sumatra. The seismic density of Mediterranean Sea area is relatively smaller.

The kernel density analysis result of historical tsunamis is shown in Fig. 7. The regions with the highest density include the Japan-Taiwan-Philippines area, western water of Sumatra and the Mediterranean region. Compared with the analysis results of

Fig. 6, there are not many earthquakes in the Mediterranean region, but the number of tsunamis is relatively bigger. Both the earthquake density and tsunami density in Japan-Taiwan-Philippines area are relatively higher.

3 Occurrence regularity of tsunamis

3.1 Analysis of source parameters

The generation of tsunamis is affected by several factors such as seismic parameters and water depth. Not all submarine earthquakes can trigger tsunamis. To explore the occurrence regularity of tsunami on the Maritime Silk Road, this paper analyzed the historical tsunamis from three source parameters, including seismic magnitude, focal depth and water depth. Tsunami data is from the global historical tsunami database of NGDC. Figure 8 shows the seismic magnitude of tsunamis on the Maritime Silk Road. It can be seen from the figure that the seismic magnitudes are generally greater than 6, most of which are concentrated between 6 and 8.

To explore whether a bigger earthquake can trigger bigger tsunami, the relationship between magnitude and tsunami wave run-up is analyzed, as shown in Fig. 9. Seen from this figure, the tsunami wave run-up shows an increasing trend with the increase of magnitude. The maximum tsunami run-up is 50.9 m of 2004 Indian Ocean tsunami, followed by 38.9 m of 2011 Japan tsunami.

Focal depth is the vertical distance from hypocenter to epicenter. It is an important parameter of seismic source, which is of great significance to understand the tectonic background of energy accumulation and release. An earthquake with a depth less than 60 kilometers is usually called shallow earthquake. Figure 10 shows the focal depth statistics of tsunami earthquakes on the

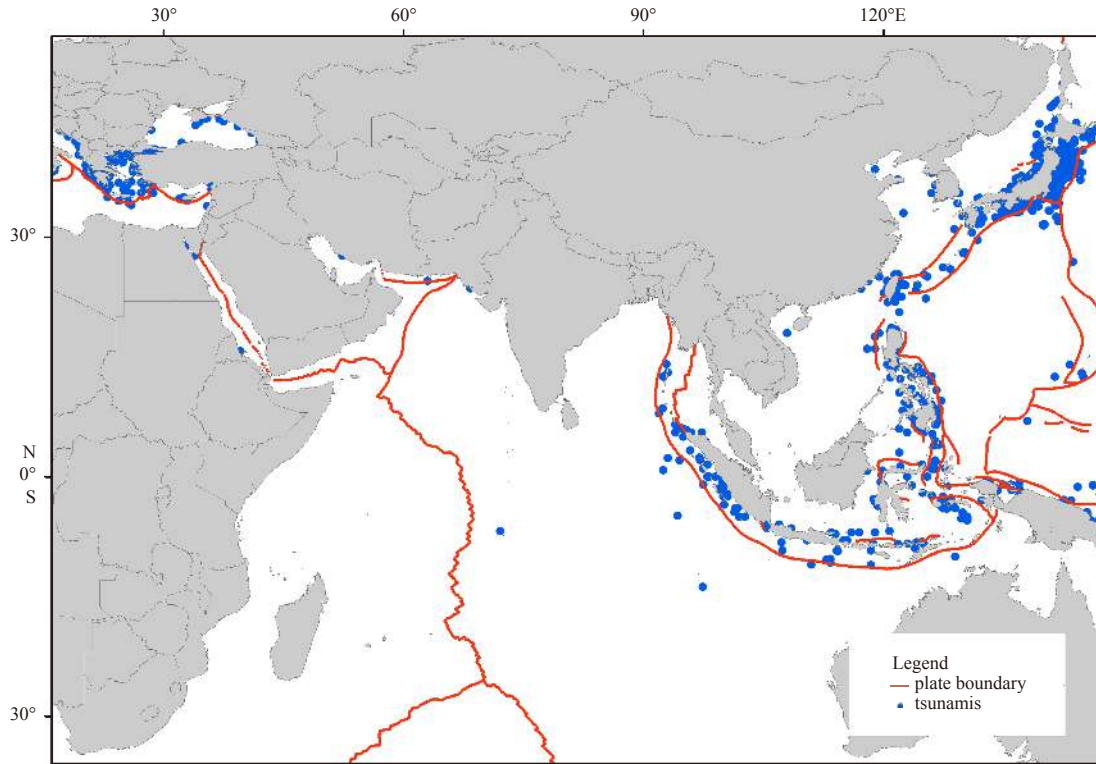


Fig. 4. Spatial distribution of tsunamis.

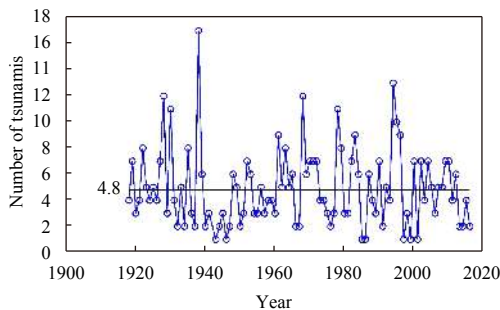


Fig. 5. Annual tsunamis on the Maritime Silk Road.

Maritime Silk Road. According to this figure, most of the earthquakes that caused tsunamis are shallow earthquakes.

It is generally believed that earthquakes with shallow water depth do not trigger tsunami. Water depth at the location of submarine earthquake is an important factor affecting the tsunami generation. The energy released by an earthquake needs a big enough water body to generate tsunami. To find out the water depth characteristics of tsunamis on the Maritime Silk Road, this paper extracted the water depth at the location of tsunami earthquakes, as shown in Fig. 11. In the figure, the water depths of tsunami sources are less than 9 000 m, most of which are distributed within 3 000 m. The water depth values of the major tsunami events on the Maritime Silk Road from 1917 to 2017 are shown in Table 1. The maximum tsunami runups of these tsunami events in Table 1 are all greater than 10 m. The tsunami events in the table are arranged according to the depth of the water. Seen from this table, the water depths of major tsunamis are between 1 000 and 4 000 m.

3.2 Analysis of tsunami probability

Generally, the earthquake with bigger magnitude has the higher probability of triggering a tsunami. However, the probability of tsunami caused by different magnitudes is still unclear. Therefore, this paper used Bayes' theorem to study the tsunami probability on the Maritime Silk Road.

Bayes' theorem is proposed by British scholar Thomas Bayes in 18th century, which can solve the conditional probability of random variables (Liu et al., 2017). In some probability events, Bayes' theorem analysis results can modify some existing conclusions. It is mainly based on the prior knowledge of conditions related to the event (Gorsevski et al., 2003). In the case of tsunami probability, the tsunami probability of different magnitudes can instruct the tsunami warning and risk assessment, which is of great significance for tsunami disaster mitigation. The equation of this theorem is as follows:

$$P(A|B) = \frac{P(AB)}{P(B)} = \frac{P(B|A)P(A)}{P(B)}. \quad (2)$$

In the Eq. (2), A and B are random events. $P(A)$ and $P(B)$ are the probabilities of A and B independently of each other. $P(A|B)$ is the probability of A given B . Because each fault has its own geological structure, the tsunami probability is different. In this paper, 8 major faults on the Maritime Silk Road are studied to discuss the tsunami probability of different magnitudes.

The probability analysis result (Table 2) shows that all earthquakes with magnitude above 8.0 can trigger tsunami. On average, the probability of an $M(5.0-5.9)$ earthquake triggering a tsunami is less than 1%; the probability of an $M(6.0-6.9)$ earthquake triggering a tsunami is around 10%; and the probability of an $M(7.0-7.9)$ earthquake triggering a tsunami is almost

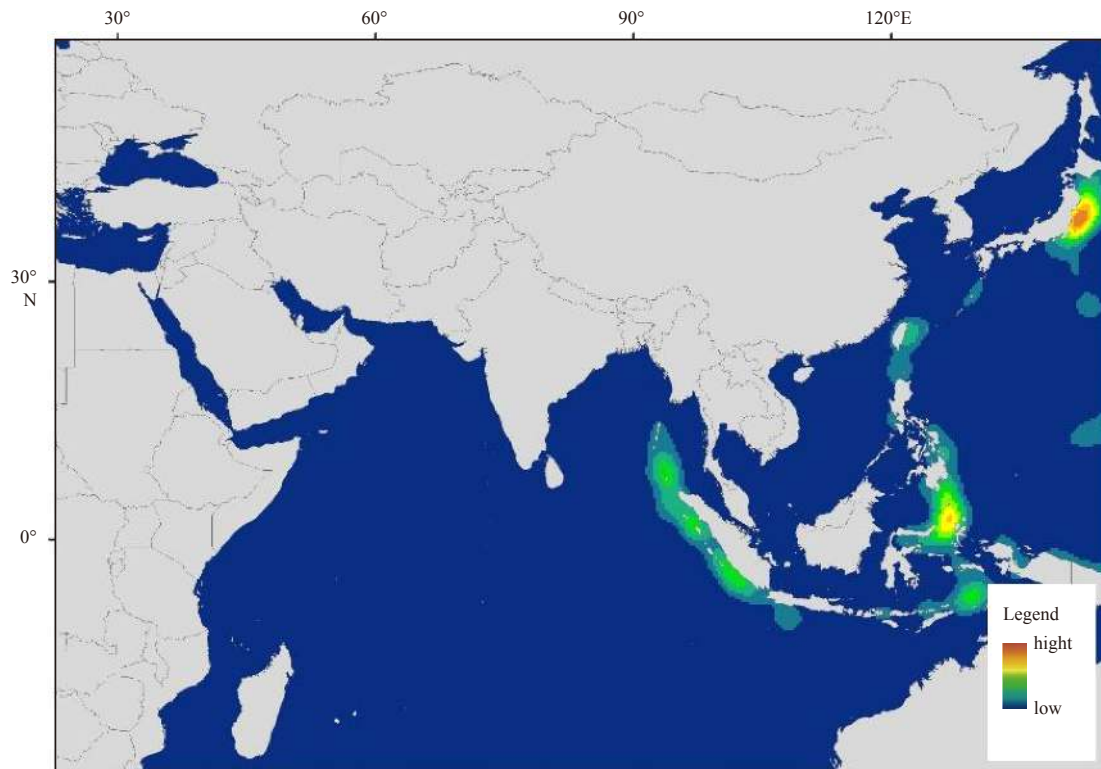


Fig. 6. Kernel density of historical earthquakes.

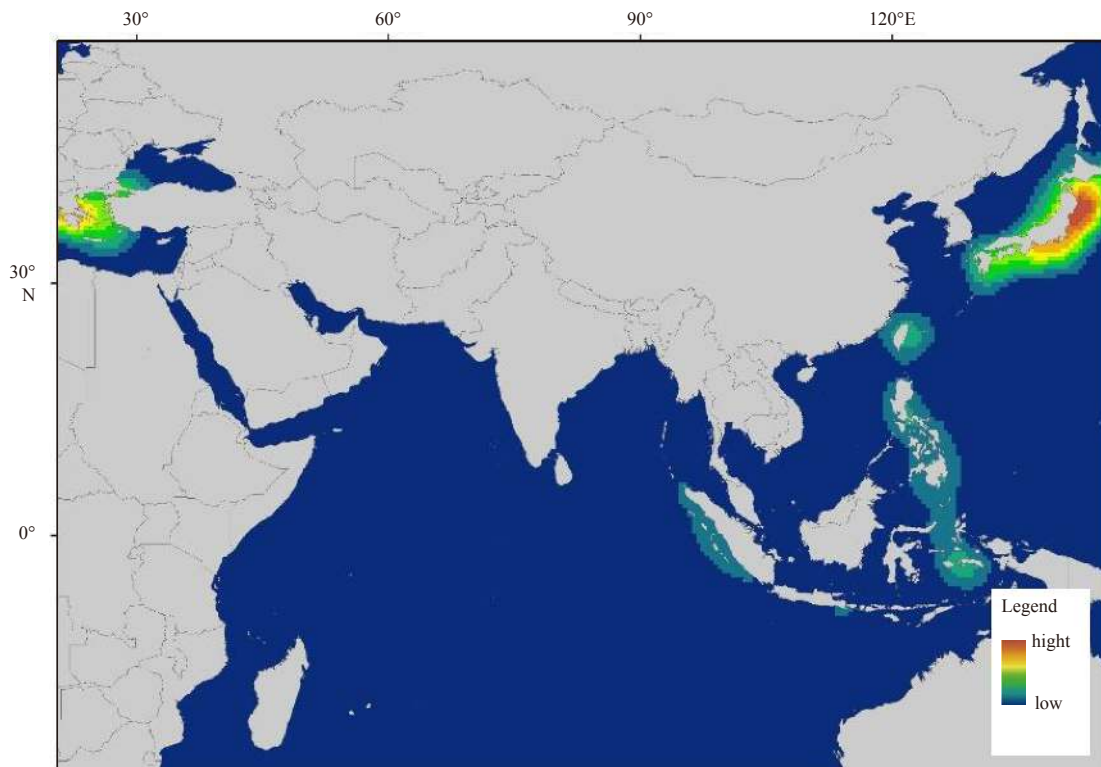


Fig. 7. Kernel density of historical tsunamis.

30%–40%. In Japan Trench, the tsunami probability of earthquakes with magnitude above 7.0 is 100.0%. According to the comparison of 8 trenches, earthquakes in Japan Trench are more likely to trigger tsunamis.

3.3 Focal mechanism solutions

Focal mechanism solution is a method of distinguishing fault types and seismogenic mechanisms. After an earthquake occurs, the focal mechanism solution can be obtained by mathematical

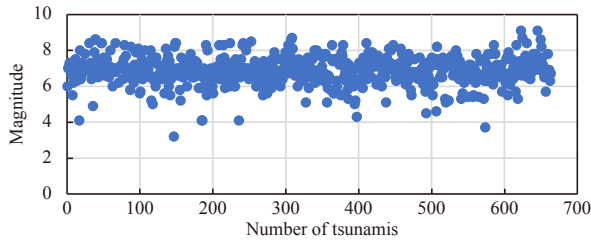


Fig. 8. Seismic magnitudes of historical tsunamis.

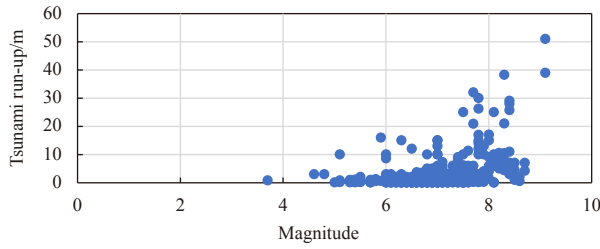


Fig. 9. Relationship between earthquake magnitudes and tsunami amplitudes.

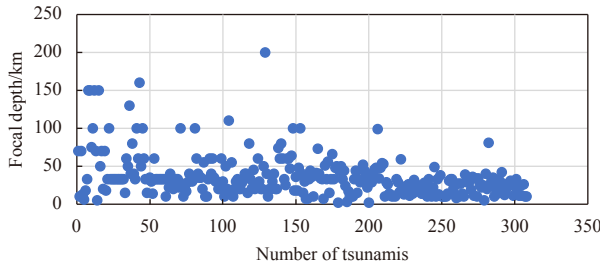


Fig. 10. Focal depths of historical tsunamis.

analysis of the seismic wave signals received by different seismic stations. The focal mechanism solution can not only make people understand the types of fault, but also reveal the specific motion of the seismic fault. The plate collision motion at the oceanic trench is complex. However, large plates have a general direction of movement. Generally, there is a typical source mechanism solution of large trench where tsunami occurs. This paper carried out statistical analysis on the focal mechanism solution using the Global Centroid Moment Tensor database, and gave the average of typical focal mechanism solutions of 8 main tec-

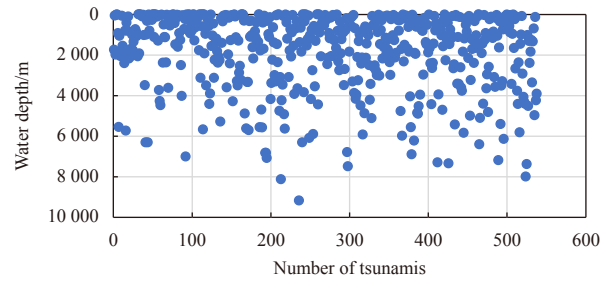


Fig. 11. Water depths of historical tsunamis.

tonic faults, as shown in Table 3. There are 5 trenches with the percentage of typical focal mechanism solutions more than 50%. The percentage of typical focal mechanism solution in Japan Trench is the highest, 83.3%. The typical value of the focal mechanism solution can reflect the general rupture of the fault, which is helpful to tsunami warning and tsunami disaster mitigation.

4 Tsunami hazard analysis

Numerical simulation is an important method in tsunami research. It can show the impact extent of some potential tsunamis and help people understand the tsunami hazard in advance (Ren et al., 2017). Some tsunami numerical models can simulate the whole lifespan of tsunami from generation, propagation, to inundation, based on the physical characteristics of tsunami waves.

The FUNWAVE model with Boussinesq equation was used in this paper, which had been validated by scholars (Shi et al., 2012). In recent years, many scholars had applied the Boussinesq equation to tsunami numerical computation. Peregrine et al. (1967) derived the standard Boussinesq equation with variable depth, according to the average depth velocity and free surface displacement. Compared with the shallow water equations, the Boussinesq equation take the frequency dispersion into account (Wang and Liu, 2006). It is shown that the numerical results obtained by using this equation are consistent with field data. The Boussinesq equation used in FUNWAVE model is as follows:

$$H_t + \frac{1}{r_0 \cos \theta} \left\{ (Hu_\alpha)_\phi + (Hv_\alpha \cos \theta)_\theta \right\} + \frac{1}{r_0^2 \cos \theta} \left[h \left(\left(z_\alpha + \frac{1}{2}h \right) A_\phi + \left(\frac{z_\alpha^2}{2} - \frac{h^2}{6} \right) B_\phi \right) \right]_\phi + \frac{1}{r_0^2} \left[h \cos \theta \left(\left(\left(z_\alpha + \frac{1}{2}h \right) A_\theta + \left(\frac{z_\alpha^2}{2} - \frac{h^2}{6} \right) B_\theta \right) \right) \right]_\theta \right\} = 0, \tag{3}$$

Table 1. Water depths and runups of historical tsunamis

Year	Focal depth/km	Magnitude	Country	Latitude	Longitude	Tsunami run-up/m	Water depth/m
1933	35	8.4	Japan	39.224°N	144.622°E	29.0	-4 124
1977	33	8.0	Indonesia	11.085°S	118.464°E	15.0	-3 978
2006	34	7.7	Indonesia	9.254°S	107.411°E	20.9	-3 522
1994	18	7.8	Indonesia	10.477°S	112.835°E	13.9	-3 440
2006	10	8.3	Japan	46.592°N	153.266°E	21.9	-3 310
1993	17	7.7	Japan	42.851°N	139.197°E	32.0	-2 881
1983	24	7.8	Japan	40.462°N	139.102°E	14.9	-2 632
2010	20	7.8	Indonesia	3.487°S	100.082°E	16.9	-2 373
1992	28	7.8	Indonesia	8.48°S	121.896°E	26.2	-2 285
1956	20	7.8	Greece	36.90°N	26.000°E	30.0	-1 471
2004	30	9.1	Indonesia	3.316°N	95.854°E	50.9	-1 062
2011	30	9.1	Japan	38.297°N	142.372°S	38.9	-1 002

Table 2. The probability of different magnitudes

Trenches	$M(5.0-5.9)$ /%	$M(6.0-6.9)$ /%	$M(7.0-7.9)$ /%	$M(8.0-8.9)$ /%	$M>9.0$ /%
Japan Trench	0.2	14.8	100.0	100.0	100.0
Java Trench	0.1	3.9	34.8	100.0	100.0
Nankai Trough	0.2	7.1	40.1	100.0	-
Ryukyu Trench	0.1	4.1	39.5	100.0	-
Philippine Trench	0.2	3.3	37.8	100.0	-
Manila Trench	0.6	11.9	41.7	-	-
Hellenick Trench	0.9	13.6	43.3	-	-
Mariana Trench	-	5.6	14.3	-	-

Table 3. The typical focal mechanism solutions of tectonic faults

Trenches	Strike/(°)	Dip/(°)	Slip/(°)	Percentage/%
Japan Trench	205	21	88	83.3
Java Trench	307	22	101	62.5
Nankai Trough	251	26	79	66.8
Ryukyu Trench	41	28	-67	41.4
Philippine Trench	160	31	72	76.2
Manila Trench	162	33	-146	46.2
Hellenick Trench	265	35	-50	57.1
Mariana Trench	201	34	-96	43.5

$$u_{\alpha t} - f v_{\alpha} + \frac{1}{r_0 \cos \theta} u_{\alpha} u_{\alpha \phi} + \frac{1}{r_0} v_{\alpha} u_{\alpha \theta} + \frac{g}{r_0 \cos \theta} \eta_{\phi} + \frac{1}{r_0^2 \cos \theta} \left\{ z_{\alpha} A_{t\phi} + \frac{z_{\alpha}^2}{2} B_{t\phi} \right\} + \frac{C_d}{H} |U_{\alpha}| u_{\alpha} = 0, \quad (4)$$

$$v_{\alpha t} + f u_{\alpha} + \frac{1}{r_0 \cos \theta} u_{\alpha} v_{\alpha \phi} + \frac{1}{r_0} v_{\alpha} v_{\alpha \theta} + \frac{g}{r_0} \eta_{\theta} + \frac{1}{r_0^2} \left\{ z_{\alpha} A_{t\theta} + \frac{z_{\alpha}^2}{2} B_{t\theta} \right\} + \frac{C_d}{H} |u_{\alpha}| u_{\alpha} = 0, \quad (5)$$

where C_d represents the drag coefficient, and θ and ϕ are latitude and longitude respectively. r_0 is the Earth's radius, and f is Coriolis. $H = h + \eta$ is the total water depth, and u_{α} and v_{α} represent the velocity in the east and north direction respectively.

In this paper, 8 potential tsunami sources of major tectonic faults were assumed and simulated by the FUNWAVE model. The locations of hypothesized tsunami sources are shown in Table 4. The input bathymetry data is the ETOPO data with the grid resolution of 2 arc minutes. The coastline of the bathymetry data has been revised using Landsat imagery. And the source parameters used in the tsunami numerical calculations are based on Table 3. In order to analyze the maximum possible tsunami wave on the Maritime Silk Road, the magnitudes of these potential tsunami sources were set as 9.0.

Table 4. Locations of potential tsunamis

Trenches	Locations	Magnitude (M_w)
Japan Trench	38.103°N, 142.86°E	9.0
Nankai Trough	31.833°N, 133.50°E	9.0
Ryukyu Trench	25.68°N, 128.81°E	9.0
Mariana Trench	12.50°N, 142.50°E	9.0
Philippine Trench	13.70°N, 125.33°E	9.0
Manila Trench	14.47°N, 119.17°E	9.0
Java Trench	3.32°N, 95.85°E	9.0
Hellenick Trench	35.50°N, 26.00°E	9.0

To show the tsunami hazard of the Maritime Silk Road more clearly, the maximum amplitude of 8 potential tsunamis was superimposed. Each grid point takes the maximum value. The result is shown in Fig. 12. As shown in this figure, many areas on the Maritime Silk Road face serious tsunami threat. The most dangerous tsunami sources are the Ryukyu Trench, Manila Trench, Java Trench and Hellenick Trench. These potential major tsunamis will affect not only the area around the source, but also the other side of the waters. The maximum tsunami amplitude on the coast of the Maritime Silk Road can reach 7 m. Some tsunamis can spread to neighboring countries in a very short time. For example, if a large tsunami occurs in the Manila Trench, the tsunami wave can spread to the entire South China Sea coast in 3 hours, which puts forward higher requirements for tsunami warning and disaster mitigation. A tsunami could affect many countries along the ocean coast, so it is necessary to strengthen international cooperation to cope with the tsunami disaster. In addition, the tsunami may cause some secondary disasters such as fires, gas leaks, explosions, radioactive pollution, and landslides. The catastrophic impact of the tsunami should cause concern.

Based on the maximum amplitude superposition of potential tsunamis in Fig. 12, this paper classifies the tsunami hazard of the Maritime Silk Road. The classification criteria is shown in Table 5, according to the warning levels of the Pacific Tsunami Warning Center. The classification result of Fig. 13 shows the tsunami hazard on the Maritime Silk Road. The tsunami hazard was divided into Level 1, 2, 3 and 4. The areas with tsunami hazard level 1 includes the Japan coast, the coast of the South China Sea, the western coast of the Java and the Mediterranean coast. The coast of the East China and the Bay of Bengal coast is level 2 of tsunami hazard. There are 68 cities with more than 100 000 people within 10 km of the coastline of tsunami hazard Level 1. The total affected population is about 129 million. The nuclear power plants, large chemical plants and other dangerous goods areas in this region are exposed to major tsunami hazard. Therefore, it is necessary to carry out tsunami hazard assessment and risk investigation in advance.

5 Discussion

The 21st century Maritime Silk Road was proposed to develop mutually beneficial cooperation and promote common prosperity. The tsunami disaster should be understood to ensure the economic and cultural exchanges on the Maritime Silk Road. The analysis result shows that tsunamis mainly occur in large faults, each of which has different tsunami occurrence regularity. The tsunami analysis of specific fault needs to be combined with the focal mechanism solution of earthquakes.

Tsunami waves can travel across the ocean, causing disastrous effects in areas far from the source. Therefore, the tsunami hazard in the entire waters should be considered. It is necessary to strengthen international cooperation and technical exchanges for the tsunami early warning service along the Maritime Silk Road. There is also a need to strengthen observation network construction and observation data sharing. Tsunami warning exercise should be held irregularly to improve the efficiency of tsunami warning agencies and government departments. In addition, tsunami awareness and education are also very important. In this paper, the numerical model was used to demonstrate the tsunami hazard levels of the Maritime Silk Road coast. However, the vulnerability of countries along the Maritime

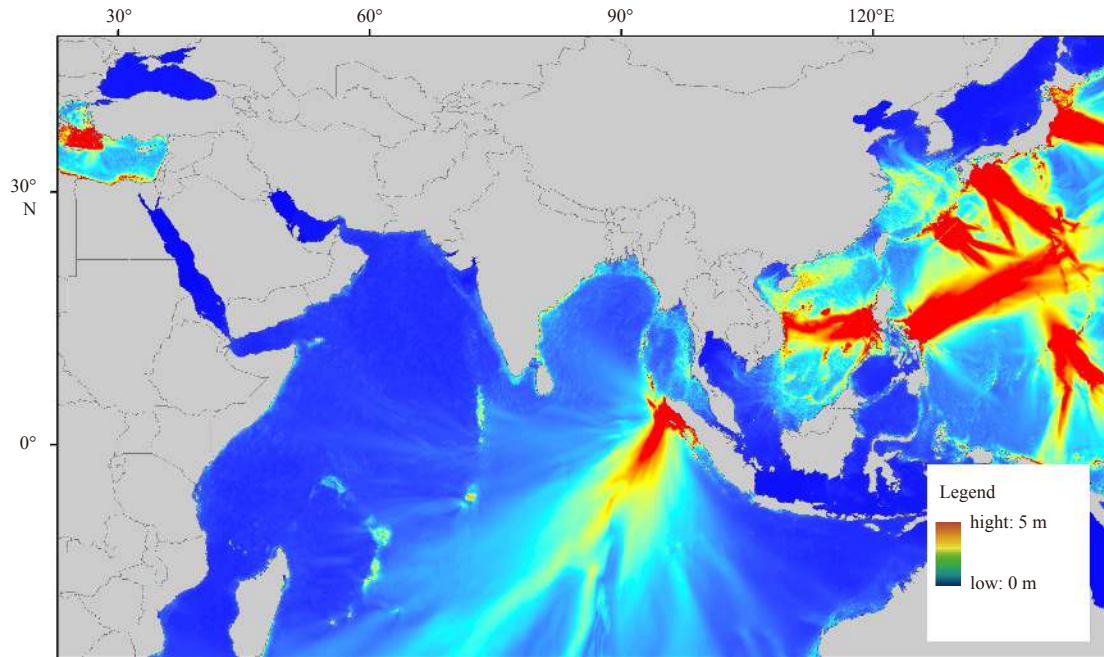


Fig. 12. Maximum amplitude superposition of potential tsunamis.

Table 5. Tsunami hazard classification

Tsunami amplitude/m	Hazard level	Color
>3	1	Red
1–3	2	Orange
0.3–1	3	Yellow
<0.3	4	Blue

Silk Road is diverse from each other. Further tsunami disaster impact analysis is worth studying in the future.

6 Conclusion

This paper studied the spatiotemporal distribution and occurrence regularity of tsunami disaster on the Maritime Silk Road based on the historical earthquake and tsunami events. The

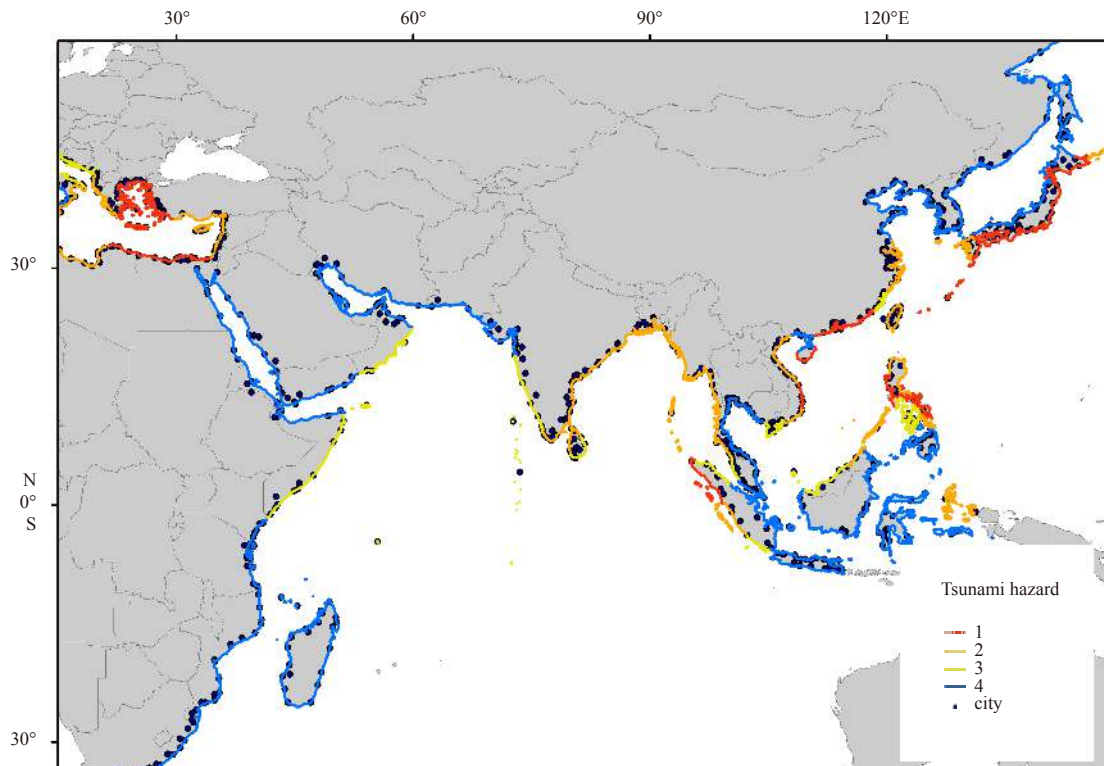


Fig. 13. Tsunami hazard levels along the Maritime Silk Road.

tsunamis on the Maritime Silk Road mainly occurred in 8 major tectonic faults, and the annual tsunamis fluctuated over time. The tsunami occurrence regularity is studied from the aspects of magnitude, focal depth and water depth. It was found that the seismic magnitudes of the tsunami sources were between 6 and 8, and the water depths of the major tsunamis were between 1 000 to 4 000 m. Most earthquakes that triggered tsunamis were shallow earthquakes. The Bayes' theorem analysis result showed the tsunami probability of different magnitudes.

Eight potential tsunami sources were hypothesized and simulated by numerical model. The calculation results were classified to show the tsunami hazard. The regions most heavily affected by the potential tsunamis include the Japan coast, the coast of the South China Sea, the western coast of the Java and the Mediterranean coast. The Japan Trench and Java Trench were the major tsunami sources on the Maritime Silk Road. In addition, the earthquakes of the Ryukyu Trench, Manila Trench and Hellenic Trench should also be concerned.

References

- Cai Xuejiao, Wu Zhifeng, Cheng Jiong. 2013. Using kernel density estimation to assess the spatial pattern of road density and its impact on landscape fragmentation. *International Journal of Geographical Information Science*, 27(2): 222–230, doi: [10.1080/13658816.2012.663918](https://doi.org/10.1080/13658816.2012.663918)
- Dao M H, Tkalic P, Chan E S, et al. 2009. Tsunami propagation scenarios in the South China Sea. *Journal of Asian Earth Sciences*, 36(1): 67–73, doi: [10.1016/j.jseaes.2008.09.009](https://doi.org/10.1016/j.jseaes.2008.09.009)
- Gorsevski P V, Gessler P E, Jankowski P. 2003. Integrating a fuzzy k -means classification and a Bayesian approach for spatial prediction of landslide hazard. *Journal of Geographical Systems*, 5(3): 223–251, doi: [10.1007/s10109-003-0113-0](https://doi.org/10.1007/s10109-003-0113-0)
- Grilli S T, Ioualalen M, Asavanant J, et al. 2007. Source constraints and model simulation of the December 26, 2004, Indian Ocean tsunami. *Journal of Waterway, Port, Coastal, and Ocean Engineering*, 133(6): 414–428, doi: [10.1061/\(ASCE\)0733-950X\(2007\)133:6\(414\)](https://doi.org/10.1061/(ASCE)0733-950X(2007)133:6(414))
- Guan K C. 2016. *The maritime silk road: history of an idea*. Pasir Panjang, Singapore: ISEAS
- Hébert H, Schindelé F, Heinrich P. 2001. Tsunami risk assessment in the Marquesas Islands (French Polynesia) through numerical modeling of generic far-field events. *Natural Hazards and Earth System Sciences*, 1(4): 233–242, doi: [10.5194/nhess-1-233-2001](https://doi.org/10.5194/nhess-1-233-2001)
- Hou Jingming, Li Xiaojuan, Yuan Ye, et al. 2016. Tsunami hazard assessment along the Chinese mainland coast from earthquakes in the Taiwan region. *Natural Hazards*, 81(2): 1269–1281, doi: [10.1007/s11069-015-2133-8](https://doi.org/10.1007/s11069-015-2133-8)
- IOC. 2013. *A Pacific-wide tsunami warning and enhanced products exercise*. Paris: IOC
- Liu Rui, Chen Yun, Wu Jianping, et al. 2017. Integrating entropy - based naïve Bayes and GIS for spatial evaluation of flood hazard. *Risk Analysis*, 37(4): 756–773, doi: [10.1111/risa.12698](https://doi.org/10.1111/risa.12698)
- Liu Yingchun, Santos A, Wang S M, et al. 2007. Tsunami hazards along Chinese coast from potential earthquakes in South China Sea. *Physics of the Earth and Planetary Interiors*, 163(1–4): 233–244, doi: [10.1016/j.pepi.2007.02.012](https://doi.org/10.1016/j.pepi.2007.02.012)
- Mao Xianzhong, Zhu Qian, Wei Yong. 2015. Risk analysis of potential regional earthquake tsunami on the coast of Zhejiang Province. *Haiyang Xuebao (in Chinese)*, 37(3): 37–45
- National Geophysical Data Center (NGDC). 2018. NOAA/WDS global historical tsunami database. Washington DC, USA. https://www.ngdc.noaa.gov/hazard/tsu_db.shtml [2018-06-07]
- Peregrine D H. 1967. Long waves on a beach. *Journal of Fluid Mechanics*, 27(4): 815–827, doi: [10.1017/S0022112067002605](https://doi.org/10.1017/S0022112067002605)
- Ren Zhiyuan, Yuan Ye, Wang Peitao, et al. 2017. The September 16, 2015 M_w 8.3 Illapel, Chile Earthquake: characteristics of tsunami wave from near-field to far-field. *Acta Oceanologica Sinica*, 36(5): 73–82, doi: [10.1007/s13131-017-1005-3](https://doi.org/10.1007/s13131-017-1005-3)
- Shi Fengyan, Kirby J T, Harris J C, et al. 2012. A high-order adaptive time-stepping TVD solver for Boussinesq modeling of breaking waves and coastal inundation. *Ocean Modelling*, 43–44: 36–51, doi: [10.1016/j.ocemod.2011.12.004](https://doi.org/10.1016/j.ocemod.2011.12.004)
- United States Geological Survey (USGS). 2018. Search earthquake catalog. Washington DC, USA. <https://earthquake.usgs.gov/earthquakes/search/> [2018-06-07]
- Wang Gang, Hu Jian, Wang Peitao, et al. 2018. Analytical and numerical investigation of tsunami trapped waves over a hyperbolic-cosine squared ocean ridge. *Haiyang Xuebao (in Chinese)*, 40(5): 15–23
- Wang Benlong, Liu Hua. 2006. Solving a fully nonlinear highly dispersive Boussinesq model with mesh-less least square - based finite difference method. *International Journal for Numerical Methods in Fluids*, 52(2): 213–235, doi: [10.1002/flid.1175](https://doi.org/10.1002/flid.1175)
- Wei Yong, Chamberlin C, Titov V V, et al. 2013. Modeling of the 2011 Japan tsunami: lessons for near-field forecast. *Pure and Applied Geophysics*, 170(6–8): 1309–1331, doi: [10.1007/s00024-012-0519-z](https://doi.org/10.1007/s00024-012-0519-z)
- Wen Yanlin, Zhu Yuanqing, Song Zhiping, et al. 2008. Preliminary numerical simulation of potential earthquake-induced tsunami in East China Sea. *Acta Seismologica Sinica*, 21(5): 456–463, doi: [10.1007/s11589-008-0456-1](https://doi.org/10.1007/s11589-008-0456-1)
- Zhao Xi, Liu Hua, Wang Benlong. 2013. Evolvement of tsunami waves on the continental shelves with gentle slope in the China Seas. *Theoretical and Applied Mechanics Letters*, 3(3): 032005, doi: [10.1063/2.1303205](https://doi.org/10.1063/2.1303205)
- Zhou Qinghai, Adams W M. 1988. Tsunami risk analysis for China. *Natural Hazards*, 1(2): 181–195, doi: [10.1007/BF00126614](https://doi.org/10.1007/BF00126614)